Available online at www.sciencedirect.com
SCIENCE DIRECT
Nuclear Instruments and Methods in Physics Research A 552 (2005) 124–130
NUCLEAR INSTRUMENTS & METHODS IN PHYSICS RESEARCH Section A
www.elsevier.com/locate/nima

High energy proton damage effects in thin high resistivity FZ silicon detectors

E. Fretwurst[a,*], L. Andricek[b], F. Hönniger[a], G. Kramberger[c], G. Lindström[a], G. Lutz[b], M. Reiche[d], R.H. Richter[b], A. Schramm[a]

[a]Institute for Experimental Physics, University of Hamburg, D- 22761 Hamburg, Germany
[b]Max-Planck-Institute, Semiconductor Laboratory, D-81739 Munich, Germany
[c]Jozef Stefan Institute, Department of Physics, University of Ljubljana, Ljubljana, Slovenia
[d]Max-Planck-Institute of Microstructure Physics, D-06120 Halle, Germany

Available online 1 July 2005

Abstract

The proposed luminosity upgrade of the Large Hadron Collider (S-LHC) will demand the inner most layers of the vertex detector to sustain fluences of about 10^{16} charged hadrons/cm^2. Due to the high multiplicity of tracks, the required spatial resolution and the extremely harsh radiation field thin silicon detector assemblies are proposed as a possible solution for this challenge. The radiation tolerance of 50 μm thin high resistivity float zone (FZ) devices has been studied for 24 GeV/c protons in the fluence range between $4\times10^{13}\,\text{cm}^{-2}$ and $8.6\times10^{15}\,\text{cm}^{-2}$. For the manufacturing of such thin devices, a technology based on direct wafer bonding and deep anisotropic etching was used. Annealing measurements at 80 °C have shown that the introduction rate g_C in the stable damage component is about the same as observed for oxygen enriched FZ detectors and that the fluence dependence of the reverse annealing amplitude N_Y exhibits a saturating function. It is also demonstrated that the annealing behavior of the reverse current related damage parameter α is independent on the fluence and the silicon material parameters. Charge collection efficiency (CCE) measurements were performed using 5.8 MeV α-particles. After fully annealing for about 31 days at 80 °C CCE was determined by extrapolation to be 66% at 10^{16} p/cm^2.

PACS: 29.40.Wk; 61.82.Fk; 85.30.De

Keywords: Silicon detectors; Wafer bonding; Radiation damage; Proton radiation

1. Introduction

Thin silicon detector assemblies are mandatory for vertex detectors in high-energy physics experiments at future colliders, in particular for the

*Corresponding author. Tel.: +49 40 8998 2956; fax: +49 40 8998 2959.
E-mail address: eckhart.fretwurst@desy.de (E. Fretwurst).

0168-9002/$ - see front matter © 2005 Elsevier B.V. All rights reserved.
doi:10.1016/j.nima.2005.06.019

proposed luminosity upgrade of the Large Hadron Collider at CERN (S-LHC) or the International Linear Collider (ILC) [1–3]. Especially the upgrade of the LHC will demand the inner most layers of the vertex detector to sustain fluences of about 10^{16} charged hadrons/cm^2 and doses up to 420 Mrad [4]. Due to the required very high rate capability and spatial resolution small area pixel detectors are the logical choice. Although there are several proposals for possible radiation tolerant semiconductor materials under investigation in the frame of the RD50 collaboration [5,6], silicon is still regarded to be the optimal choice because of the very high material quality and the best developed device technology.

A considerable reduction of the pixel area, essential for the inner layers of the vertex detector, allows correspondingly a smaller detector thickness while maintaining the same input capacitance and hence its influence on the electronic noise. In addition, the shot noise due to the leakage current will be reduced and thin active layers will certainly reduce the voltage for total depletion. This allows to establish a high electric field strength throughout the sensitive volume and the degradation of the charge collection efficiency due to trapping can be partly compensated.

For the development of thin detectors different technological approaches are possible and under investigation in the frame of the RD50 collaboration. These are thin epitaxial layers grown on highly doped Czochralski substrates [7], thinning of high resistivity float zone (FZ) devices by chemical etching [8] and processing of thin high resistivity FZ devices using the so-called wafer bonding technology [9]. In this work we present results on the radiation hardness of 50 μm thick devices manufactured on high resistivity n-type FZ silicon using the wafer bonding technology [9].

2. Experimental procedures

The technological approach to manufacture very thin sensors is based on the wafer bonding technique. The process starts with two oxidized wafers, the sensor wafer (top wafer) and the so-called handle wafer. The backside implantation of the top wafer is also done before bonding. These two wafers are then bonded together and are annealed at high temperatures forming a stack with buried backside implants for the top wafer and silicon oxide in between. The top wafer is then thinned to the desired thickness and the front side process is performed as for a conventional wafer. After this process the backside of the handle wafer is structured and removed according to the sensor backside area and the silicon of the handle wafer is selectively etched away. Details of this technology are described in Ref. [9]. Fig. 1 shows a photograph of the front and the backside of a chip with four diodes in the four thinned windows.

The silicon material used is high resistivity (~3 kΩ cm) n-type FZ material with ⟨1 0 0⟩ orientation. The devices are p^+-n-n^+ pad diodes with an area of 10 mm^2 surrounded by a single guard ring. The thickness for the devices under investigation varies between 47 and 50 μm. According to the high resistivity and the small thickness the voltage for full depletion is only $V_{fd} \approx 2$–3 V.

The irradiation has been performed at the irradiation facility at CERN with 24 GeV/c protons. A set of nine devices was exposed in consecutive steps to fluence values between 4×10^{13} and 8.6×10^{15} cm^{-2}. In order to investigate the radiation-induced changes in the short- and long-term operation all samples underwent after irradiation an isothermal annealing procedure at 80 °C with cumulative steps up to 45000 minutes (≈31 days). After each annealing

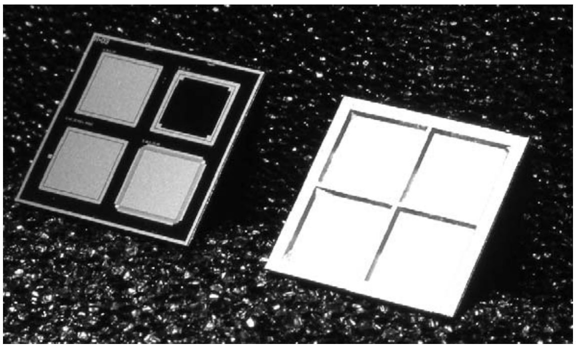

Fig. 1. Top (left) and handle wafer side (right) of a chip with four 10 mm^2 diodes on 50 μm thin silicon.

step the devices were electrically characterized at 20 °C by C–V and I–V measurements with the guard ring properly connected to ground in order to minimize lateral edge effects on both measurements. After the full annealing cycle up to the cumulated time of 31 days charge collection measurements were performed for 5.8 MeV α-particles of a ^{244}Cm-source using the same TCT-setup for recording current pulse shapes induced by laser light pulses [10].

3. Experimental results

The development of the voltage for full depletion of the devices V_{fd} as extracted from C–V measurements after annealing at 80 °C as function of fluence is shown in Fig. 2. The annealing time corresponds to values at which the annealing curve of V_{fd} or ΔN_{eff} reaches its minimal value (see Fig. 4). At the lowest fluence value of $4 \times 10^{13}\,\mathrm{cm}^{-2}$ a very small depletion voltage of 1.6 V is measured followed by a non-linear increase up to 9.0 V at $6 \times 10^{14}\,\mathrm{cm}^{-2}$. In the high fluence range up to $8.6 \times 10^{15}\,\mathrm{cm}^{-2}$ a linear increase is observed. According to former results which had been achieved for hadron induced radiation damage of thick (300 μm) high resistivity FZ silicon detectors we can assume that all devices are type inverted and that the development of the doping concentration N_{eff} with fluence Φ can be parameterized by [11,12]:

$$N_{eff} = \left|N_{eff,0} \times \exp\left(-c^{*}\Phi\right) - \beta \times \Phi\right|. \quad (1)$$

$N_{eff,0}$ is the initial doping concentration, c^* is related to the so-called donor removal constant and β the introduction rate of acceptors being negatively charged in the space charge region. From the fit to the experimental data we derive for these parameters: $c^* = 2.3 \times 10^{-14}\,\mathrm{cm}^2$ and $\beta = 3.6 \times 10^{-3}\,\mathrm{cm}^{-1}$. The β-value is in the same order as obtained for oxygen enriched FZ (DOFZ) silicon [11,13], although these devices were not subjected to any deliberate oxygenation procedure. Possibly the high temperature treatments during the wafer bonding and the device processing lead to an in-diffusion of oxygen from the oxide surface layers and may increase the oxygen concentration throughout the 50 μm thin bulk beyond the initial level of the untreated material.

For the reverse current per volume, taken at full depletion and after an annealing of 8 min at 80 °C a linear increase with accumulated fluence is observed (see Fig. 3). The extracted slope representing the current related damage parameter is $\alpha(T_a = 80\,°\mathrm{C}, t = 8\ \mathrm{min}) = 2.4 \times 10^{-17}\,\mathrm{A/cm}$ which is in agreement with results of numerous studies on various silicon materials [11–14].

Each diode underwent a full annealing cycle at 80 °C for accelerating the annealing kinetics and to study all components in the damage-induced change of the effective doping concentration ΔN_{eff}

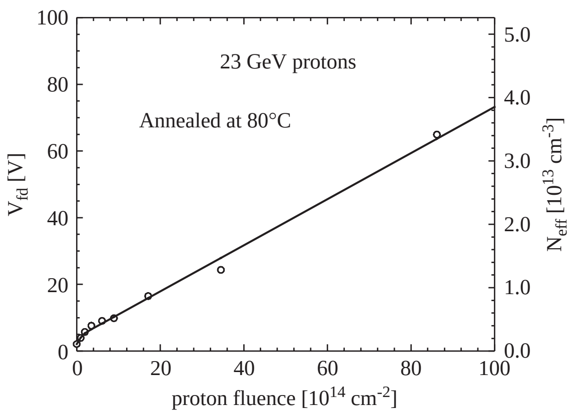

Fig. 2. Development of full depletion voltage V_{fd} as function of fluence after annealing at 80 °C for specific durations (8 min up to $1.7 \times 10^{15}\,\mathrm{cm}^{-2}$, 30 min at $3.5 \times 10^{15}\,\mathrm{cm}^{-2}$, 60 min at $8.6 \times 10^{15}\,\mathrm{cm}^{-2}$).

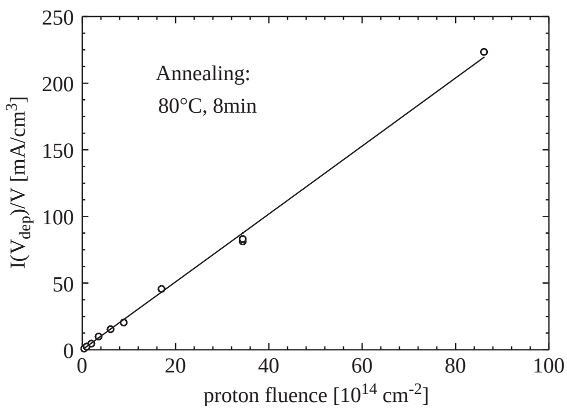

Fig. 3. Increase of reverse current per volume with fluence after annealing at 80 °C for 8 min.

with respect to its initial value before irradiation $N_{\mathrm{eff},0}$ [13]:

$$\Delta N_{\mathrm{eff}}(\Phi, t(T_a)) = N_{\mathrm{eff},0} - N_{\mathrm{eff}}(\Phi, t(T_a)). \quad (2)$$

As function of time and fluence ΔN_{eff} can be described as:

$$\Delta N_{\mathrm{eff}}(\Phi, t(T_a)) = N_A(\Phi, t(T_a)) + N_C(\Phi) + N_Y(\Phi, t(T_a)). \quad (3)$$

In this equation, it has to be emphasized that the time dependence is in itself subject to the annealing temperature T_a. The three components in Eq. (3) are: a short term annealing N_A, a stable damage part N_C and the reverse annealing component N_Y. N_C can be described by an incomplete donor removal, depending exponentially on the fluence, with a final value $N_{c,0}$, and a fluence proportional introduction of stable acceptors with a rate g_C:

$$N_C(\Phi) = N_{C,0} \times (1 - \exp(-c\Phi)) + g_C \times \Phi. \quad (4)$$

N_C should obey a similar fluence dependence as exhibited in the development of N_{eff} as function of Φ shown in Fig. 2. The time dependence of the reverse annealing component is best described by

$$N_Y(\Phi, t(T_a)) = N_{Y,\mathrm{inf}} \times \{1 - 1/(1 + t/\tau_Y(T_a))\} \quad (5)$$

where the amplitude is given by $N_{Y,\mathrm{inf}}(\Phi) = N_{Y,\mathrm{sat}} \cdot (1-\exp(-c_Y\Phi))$ which can be approximated for low fluences to $N_{Y,\mathrm{inf}} = g_Y \cdot \Phi$ (having defined $g_Y = N_{Y,\mathrm{sat}} \cdot c_Y$) and $\tau_Y(T_a)$ is the characteristic time constant of this long term process. The problems connected with this simplified model of the reverse annealing are discussed in Ref. [15].

How well this model describes the experimental data for the full set of fluences as function of the annealing time is shown in Fig. 4. The full lines are the result of fits according to the functional dependencies as described above.

From these plots it becomes obvious that the minimum of the annealing curves shifts to longer annealing times for the last two high fluence values (3.4×10^{15} and $8.6 \times 10^{15}\,\mathrm{cm}^{-2}$). This corresponds with an increase of the short-term annealing time constant and in particular a strong increase of the reverse annealing time constant τ_Y as function of Φ is observed, as demonstrated in Fig. 5. A similar dependence had been observed for DOFZ-detectors but already for lower fluences [13,16]. Furthermore, the fluence dependence of the reverse annealing amplitude $N_{Y,\mathrm{inf}}$ shows a small but not negligible saturation effect (see Fig. 6) which is also typically observed in DOFZ material [13,16]. Finally, in Fig. 6 the fluence dependence of the stable component N_C is included. The solid line presents the fit according to Eq. (4) with an introduction rate $g_C = 3.0 \times 10^{-3}\,\mathrm{cm}^{-1}$, which is very close to the extracted β-value presented above. All these findings strengthen the assumption that these devices exhibit a larger amount of oxygen as expected for standard high resistivity FZ material. The extracted parameters are summarized in Table 1 and

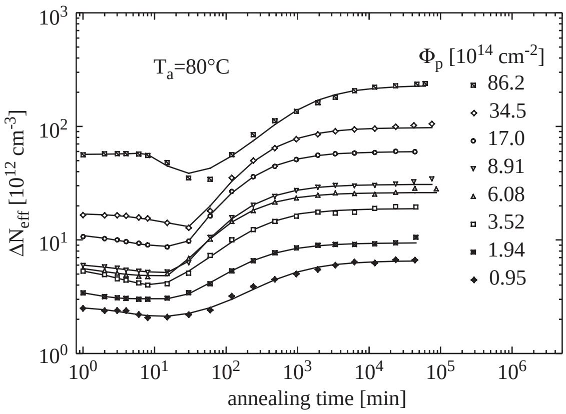

Fig. 4. Change of effective doping concentration as function of cumulated annealing time at $T_a = 80\,^{\circ}\mathrm{C}$ after irradiation with different fluences.

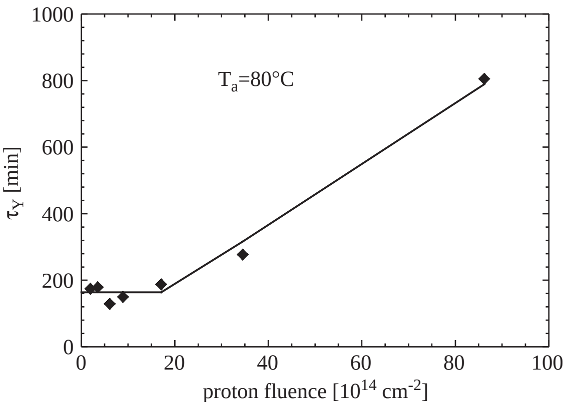

Fig. 5. Reverse annealing time constant versus proton fluence.

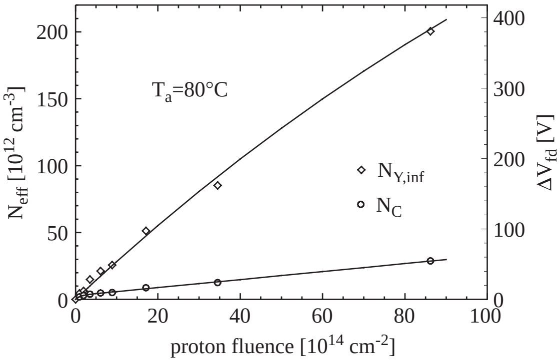

Fig. 6. Fluence dependence of the stable damage component N_C and the reverse annealing amplitude $N_{Y,inf}$.

Table 1
Damage parameters for the 50 µm FZ devices in comparison to results derived from 300 µm DOFZ samples

Parameter	50 µm FZ	DOFZ
$N_{C,0}/N_{eff,0}$	0.97	1.0
c (cm^2)[a]	1.5×10^{-14}	—
g_C (cm^{-1})[a]	4.8×10^{-3}	6.6×10^{-3}
$N_{Y,sat}$ (cm^{-3})	5.5×10^{14}	1.0×10^{13}
c_Y (cm^2)[a]	8.4×10^{-17}	4.7×10^{-15}
g_Y (cm^{-1})[a]	4.6×10^{-2}	4.8×10^{-2}
τ_Y (min)[b]	164	155

The parameters with the label
[a]are normalized to 1 MeV neutron equivalent damage, the given time constants τ_Y
[b]are only valid for low fluence values (see Fig. 5).

compared with those derived from 300 µm thick devices which had been oxygen enriched by diffusion at 1150 °C for 72 h [6,16]. However, it should be emphasized here that the damage parameters can exhibit a wide variation for standard FZ devices processed by different manufacturer or using different FZ ingots [17].

The annealing of the reverse current is shown in Fig. 7 for all irradiated diodes. The time dependence of the reverse current per volume $I_{rev}/V = \alpha(t(T_a)) \times \Phi$ is given by the time dependence of the damage parameter α, which is well described by a short term exponential decay, a constant and a logarithmic term [14]:

$$\alpha(t(T_a)) = \alpha_0 \times \exp(-t/\tau_I) + \alpha_1 - \alpha_2 \times \ln(t/t_0) \qquad (6)$$

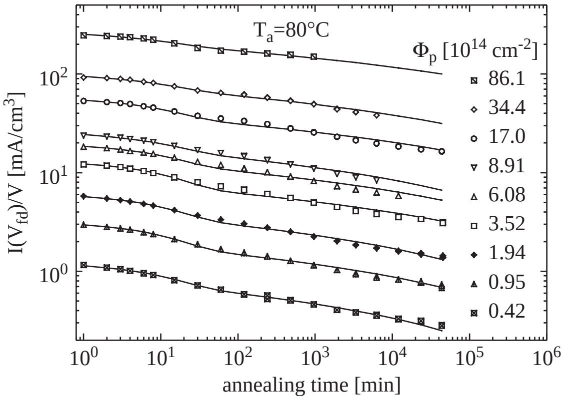

Fig. 7. Development of reverse current per volume as function of cumulated annealing time at 80 °C after irradiation with different fluences.

Table 2
Parameters for the annealing of the reverse current related damage coefficient α (Eq. (6)). $\alpha_{0,1,2}$ values normalized to 1 MeV neutrons

Parameter	This work	Ref. [14]
α_0 (10^{-17} A/cm)	1.33 ± 0.08	1.13
τ_I (min)	18 ± 2	9
α_1 (10^{-17} A/cm)	4.01 ± 0.42	4.23
α_2 (10^{-18} A/cm)	2.60 ± 0.51	2.83

where t_0 is fixed to 1 min.The extracted parameters are given in Table 2 and compared with those reported in Ref. [14]. Also in this case the values are normalized to a 1 MeV neutron equivalent damage taking a hardness factor of 0.62 for 24 GeV/c protons with respect to 1 MeV neutrons into account.

For the application of such thin devices in a radiation environment as expected for S-LHC the degradation of the charge collection efficiency due to the loss of the drifting charge carriers by trapping is the major problem. The charge collection properties of the irradiated and fully annealed diodes were measured using a collimated beam of α-particles (see Section 2). As the α-particles penetration depth is 23 µm (taking an air gap of 3 mm between the source and the detector surface into account) both holes and electrons

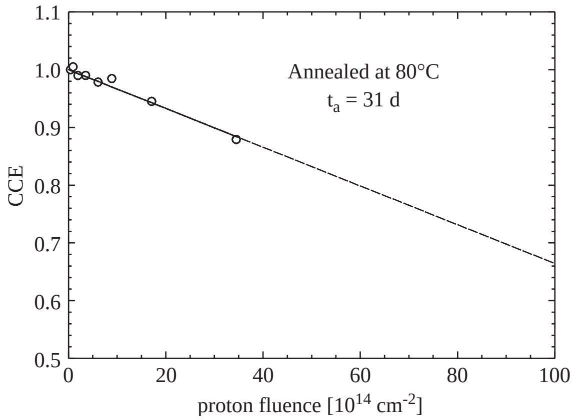

Fig. 8. Decrease of CCE with fluence after full annealing cycle at 80 °C. Measurements performed at 20 °C.

contribute to the induced charge but not equally. In Fig. 8 the measured charge collection efficiency is plotted as function of fluence. For the highest fluence value of $8.6 \times 10^{15}\,cm^{-2}$ CCE measurements were not possible because for full depletion a bias voltage as high as 425 V is needed. At such high bias voltage a soft break down in the reverse current occurred. For all other devices the CCE values correspond to a constant bias voltage of 190 V which is always above their full depletion voltage, being maximal 180 V for the device irradiated up to $3.5 \times 10^{15}\,cm^{-2}$. The solid line in Fig. 8 presents a fit to the experimental data according to: $CCE = 1 - \beta_c \times \Phi$. For the parameter β_c a value of $3.4 \times 10^{-17}\,cm^2$ is derived which leads to an extrapolated CCE value of 66% at $\Phi = 10^{16}\,cm^{-2}$ (broken line in Fig. 8). If one compares this result with charge collection measurements on proton irradiated 50 μm epitaxial devices performed with a ^{90}Sr β source (representing minimum ionizing particles) a quite similar value of 60% at $10^{16}\,cm^{-2}$ had been observed [18]. This indicates that for thin detectors charge collection measurements with α-particles result in quite similar CCE values as one would achieve with mips. Further, these observations point to a universal behavior of charge carrier trapping in highly proton irradiated silicon devices being independent on the silicon material type and the impurity content.

4. Conclusions

The presented study on high energy proton damage of thin high resistivity FZ devices validates the beneficial effects concerning the scaling of the radiation induced change of the full depletion voltage with the thickness of the active sensor layer and the reverse current. For the first time the full annealing of the effective doping concentration up to a cumulated duration of about 31 days at 80 °C could be investigated and analyzed for extremely high fluences ($8.6 \times 10^{15}\,cm^{-2}$) for high resistivity FZ devices. This was so far not possible for 300 μm thick detectors since the full depletion voltage after the final reverse annealing would exceed values of about 15 kV for fluences in the order of $10^{16}\,p/cm^2$. The extracted damage parameters for the change of the effective doping concentration indicate that the wafer bonding and device processes possibly increase the oxygen concentration in the sensitive layer leading e.g. to a reduced acceptor introduction rate g_C which is in the same order of oxygen enriched FZ material. Further, thin sensor layers allow to establish a high electric field strength in the order of 20–40 kV/cm throughout the active volume at moderate bias voltages (100–200 V) without the danger of electrical breakdown. This makes high carrier drift velocities possible, near to their saturation values, and in combination with the small thickness of 50 μm the carrier collection time is extremely short. Thus, the losses of signal charge due to trapping can be partly compensated. A further improvement of the charge collection efficiency in thin pixel devices might be possible if one chooses an n^+-n structure since then electrons would be the leading charge carriers.

References

[1] F. Giannotti, et al., hep-ph/02004087, April 2002.
[2] T. Behnke, S. Bertolucci, R.D. Heuer, R. Settles (Eds.), TESLA—Technical Design Report, Part 4: A Detector for TESLA, 2001, ISBN3-935702-00-0.
[3] N. Wermes, Nucl. Instr. and Meth. A 512 (2003) 277.
[4] M. Huhtinen, Radiation Issues for S-LHC, S-LHC Electronics Workshop, CERN, February 2004.
[5] R&D Proposal, LHCC 2002-003/P6, 15.2.2002, CERN.
[6] RD50 Status Report 2002/2003, CERN-LHCC-2003-058.

[7] G. Kramberger, D. Contarato, E. Fretwurst, F. Hönniger, G. Lindström, I. Pintilie, R. Röder, A. Schramm, J. Stahl, Nucl. Instr. and Meth. A 515 (2003) 665.
[8] S. Ronchin, M. Boscardin, G.-F. Dalla Betta, P. Gregori, V. Guarnieri, C. Piemonte, N. Zorzi, Nucl. Instr. and Meth. A 530 (2004) 134.
[9] L. Andricek, G. Lutz, M. Reiche, R.H. Richter, IEEE Trans. Nucl. Sci. NS-51 (3) (2004) 1117.
[10] E. Fretwurst, V. Eremin, H. Feick, J. Gerhardt, Z. Li, G. Lindström, Nucl. Instr. and Meth. A 388 (1997) 356.
[11] A. Ruzin, G. Casse, M. Glaser, A. Zanet, F. Lemeilleur, S. Watts, IEEE Trans. Nucl. Sci. NS-46 (5) (1999) 1310.
[12] Z. Li, B. Dezillie, M. Bruzzi, W. Chen, V. Eremin, E. Verbitskaya, P. Weilhammer, Nucl. Instr. and Meth. A 461 (2001) 126.
[13] G. Lindström, et al., Nucl. Instr. and Meth. A 466 (2001) 308.
[14] M. Moll, E. Fretwurst, M. Kuhnke, G. Lindström, Nucl. Instr. and Meth. B 186 (2002) 100.
[15] M. Moll, Ph.D.-Thesis, University of Hamburg, DESY-THESIS-1999-040, 1999, ISSN-1435-8085.
[16] G. Lindström, E. Fretwurst, F. Hönniger, I. Pintilie, R. Röder, J. Stahl, Recent Damage Results from the HH-CiS Collaboration, 1st RD50 Workshop, CERN 2.-4. October 2002.
[17] M. Moll, Nucl. Instr. and Meth. A 511 (2003) 97.
[18] G. Kramberger, V. Cindro, I. Dolenc, E. Fretwurst, G. Lindström, I. Mandić, M. Mikuž, M. Zavrtanik, contribution to the Fifth International Conference on Semiconductor Materials Detectors and Devices RESMDD04, Florence, Italy, October 10–13, 2004.